Inorganic Chemistry

Article

pubs.acs.org/IC

Cooperativity Between Low-Valent Iron and Potassium Promoters in Dinitrogen Fixation

Travis M. Figg, Patrick L. Holland,[‡,]* and Thomas R. Cundari*

Department of Chemistry and Center for Advanced Scientific Computing and Modeling (CASCaM), University of North Texas, Denton, Texas 76203-5017, United States

[‡]Department of Chemistry, University of Rochester, Rochester, New York 14627, United States

* *Supporting Information*

ABSTRACT: A density functional theory (DFT) study was performed to understand the role of cooperativity between iron- -diketiminate fragments and potassium promoters in N_2 activation. Sequential addition of iron fragments to N_2 reveals that a minimum of three Fe centers interact with N_2 in order to break the triple bond. The potassium promoter stabilizes the N^3 ligand formed upon N_2 scission, thus making the activated iron nitride complex more energetically accessible. Reduction of the complex and stabilization of N^3 by K^+ have similar impact on the energetics in the gas phase. However, upon inclusion of continuum THF solvent effects, coordination of K^+ has a reduced influence upon the overall energetics of dinitrogen fixation; thus, reduction of the trimetallic Fe complex becomes more impactful than coordination of K^+ vis-a-vis N_2 activation upon the inclusion of solvent effects.

INTRODUCTION

Conversion of dinitrogen (N_2) into useful materials is desired for uses such as the production of ammonia (NH_3), one of the most important chemicals used in synthetic fertilizers.[1] However, N_2 is difficult to activate, because of the inherent strength of the N N triple bond (235 kcal/mol). The dominant industrial method for the reductive cleavage of N_2 and formation of NH_3 is the catalytic reduction of N_2 with dihydrogen (H_2) via the Haber Bosch process. Because of its low cost, iron is commonly used to catalyze the Haber Bosch process.[2] Potassium promoters improve the catalytic activity of iron surfaces, partially because of an increase in the rate constant for N_2 dissociation on the iron surface.[3] In synthetic compounds, cooperative binding of N_2 by iron and alkali metal ions has been shown to weaken the N N bond more than iron alone, and this trend has been extended to chromium,[4] cobalt,[5,6] and nickel.[7] However, these systems do not cleave the N N bond. Further progress in cooperative N_2 activation requires better understanding of two key factors: (1) the reductive cleavage of the N_2 bond, and (2) the role of promoters such as potassium.

Recently, Holland and co-workers reported a soluble iron- -diketiminate ([Fe]) system that can cleave N_2 to give a bis(nitride) intermediate (Figure 1).[11] Relatively few Fe-nitride complexes have been reported in the literature that involve more than two Fe centers interacting with nitride atoms, and no others are derived from N_2.[12,13] The complex in Figure 1 arises from cleavage of N_2, and has three [Fe] fragments interacting directly with nitrides and a fourth [Fe] interacting indirectly through a series of Cl and K interactions. Although this system is not catalytic, the chemistry depicted in Figure 1 is a potential stepping stone to a better understanding of catalysts for solution-phase N_2 fixation.

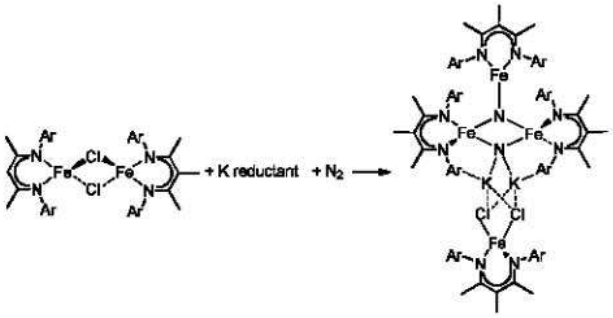

Figure 1. Structure of the soluble iron- -diketiminate-nitride complex formed upon cleavage of the N_2 triple bond. Ar = 2,6-$C_6H_3Me_2$.

In this study, density functional theory (DFT) calculations are employed to understand the role of cooperativity between multiple iron- -diketiminate fragments. For example, how many Fe atoms are needed to cleave the N_2 bond in the reduction step, and what intermediates are potentially involved? Theoretical calculations have greatly aided in understanding N N bond cleavage.[8 10] The research reported here indicates that interaction of N_2 with more metal centers increases the N N activation, and thus N_2 fixation benefits from cooperation between metals. The present calculations also yield insight into the effects of K promoters in N_2 fixation.[14]

Received: January 19, 2012
Published: June 26, 2012

   dx.doi.org/10.1021/ic300150u | Inorg. Chem. 2012, 51, 7546 7550

COMPUTATIONAL DETAILS

Density functional theory (DFT) was used to facilitate comparison between the various ground states of the $[Fe]_3N_2$ and $[Fe]_3(N)_2$ species. The Gaussian 09 software package[15] was used for geometry optimizations, and frequency calculations. The B3LYP/6-31+G(d) calculated geometries and properties of $[Fe]N_2$ and $[Fe]_2N_2$ species are similar to those previously reported from multiconfiguration self-consistent field (MCSCF) computations.[16 18] Additional continuum solvent corrections are computed in tetrahydrofuran (THF), using the SMD formulation, and are compared to the gas-phase energetics.[19] Since computations on the monometallic and bimetallic Fe- -diketiminate species have been reported previously,[16 18] the present contribution focuses on trimetallic species, the interactions of K^+ on important intermediates in an array of binding modes, and the role of reduction.

Various isomers of the $[Fe]_n$-N_2 complexes were calculated in all plausible spin states. Free energies are quoted, relative to separated starting materials: (iron- -diketiminate)$_n$ + N_2 (n = number of [Fe] fragments involved in the reaction). Bond lengths are given in Ångstroms. Initial attempts to model the tetra-iron complex in the Figure 1 molecule with ONIOM techniques revealed that the substituents need to be modeled with full QM techniques, because of the importance of K^+/ -arene interactions. The ligands were thus truncated to $C_3N_2H_5$ for computational expediency; in previous reports, we have found that this truncation gives iron-dinitrogen (Fe-N_2) complexes with metrical and spectroscopic parameters that agree well with the experiment and faithfully represents the core electronic properties of larger -diketiminate supporting ligands.[6,16 18] The studies here are limited to a single K^+ ion and three Fe atoms, because the fourth Fe atom in the complex reported by Holland et al.[11] interacts indirectly with the Fe_3N_2 core via K^+/ -arene interactions.

RESULTS AND DISCUSSION

This paper explores the effect of sequentially adding Fe- -diketiminate fragments to free N_2 in various binding modes. The experimental route to the complex in Figure 1 starts from potassium reduction of an iron(II)- -diketiminate starting material to give a presumed iron(I) species that were modeled here as the unsaturated fragment iron- -diketiminate. Previous work revealed that three-coordinate iron(I) gives strong backbonding into the * orbitals of N_2, and binding of a second fragment enhances N_2 bond lengthening.[16,18] A single [Fe] binds N_2 in an end-on (E) fashion in a quartet spin state, $G_{rel}(^4E\text{-}FeN_2)$ = 13 kcal/mol. The lowest energy bimetallic N_2 complex is end-on/end-on (EE) in a septet state, as seen experimentally for closely related compounds,[18] with $G_{rel}(^7EE\text{-}Fe_2N_2)$ = 40 kcal/mol. Binding of the second fragment is thus cooperative (defined here as the extra stabilization in a bimetallic complex beyond that expected from two monometallic interactions) by 40 (2 × 13) = 14 kcal/mol. The ligation of a second E-Fe increases the N_2 bond length by 5%, from 1.127 Å to 1.187 Å.

The key advance here is to explore the interaction of more than two iron(I) fragments with N_2, and so potential binding modes were explored for a third [Fe] fragment interacting with N_2. Three isomers of trimetallic complexes were compared: end-on/end-on/side-on (abbreviated EES-Fe_3N_2), end-on/side-on/side-on (abbreviated ESS-Fe_3N_2), and all-side-on (abbreviated SSS-Fe_3N_2). Note that [S Fe] indicates a side-on interaction of iron with N_2, which, to our knowledge, has never been observed experimentally in an iron complex; therefore, this study gives insight into the expected geometry of such an interaction. Various conformers within each family were explored; the lowest energy geometries are given in the figures.

The lowest energy neutral trimetallic isomer, Figure 2 (left), is calculated to be ^{10}EES-Fe_3N_2, G_{rel} = 62 kcal/mol, with an

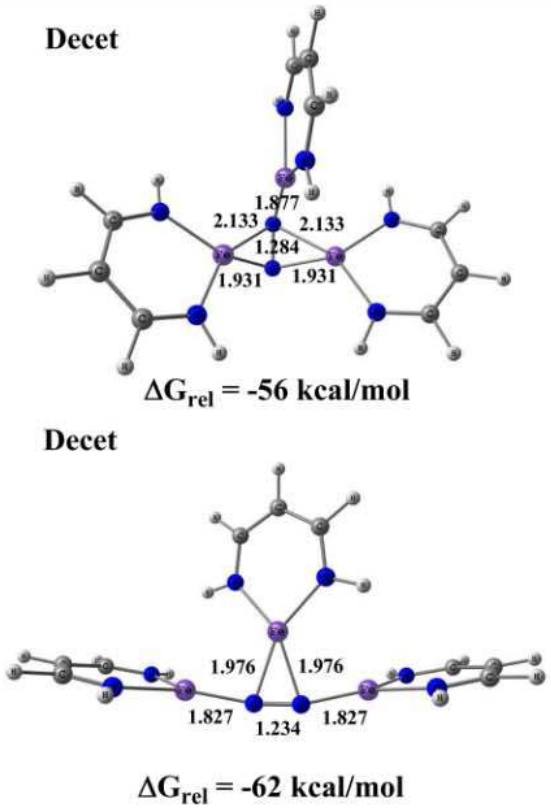

Figure 2. B3LYP geometries of ^{10}EES-Fe_3N_2 (top) and ^{10}ESS-Fe_3N_2 (bottom). The superscript numeral denotes the lowest energy multiplicity ($2S + 1$). Bond lengths given in Å. G_{rel} is calculated relative to isolated [Fe] and N_2.

N N bond length of 1.234 Å. A ^{10}ESS-Fe_3N_2 linkage isomer (Figure 2, right), d_{NN} = 1.284 Å, is only 6 kcal/mol higher than the calculated lowest energy isomer. SSS-Fe_3N_2 isomers were calculated to be thermodynamically unfavorable (by 12 kcal/mol), with respect to those in Figure 2, and, therefore, are not discussed further. Binding of the third [Fe] fragment to ^{7}EE-Fe_2N_2 to give ^{10}EES-Fe_3N_2 is found to release 22 kcal/mol, which is 5 kcal/mol less exergonic than the binding of a second [Fe] fragment to ^{4}E-FeN_2. Importantly, both EES and ESS isomers are energetically accessible, and each lengthens the N N bond significantly more than two iron fragments in ^{7}E-Fe_2N_2.

Interestingly, ^{6}ESS-$Fe_2(N)_2$, which is an isomer with a cleaved N N bond where $(N)_2$ denotes a bis(nitride) complex, was also present (Figure 3). This complex has a N···N distance of 2.598 Å and a relative G_{rel} of 40 kcal/mol. One of the two nitrides in this species is attached to only two Fe atoms. This nitride nitrogen forms an apparent double bond to one of the Fe atoms, with d_{FeN} = 1.654 Å, which is a relatively strained interaction that may explain why it is 16 kcal/mol less stable than ^{10}ESS-Fe_3N_2 (see Figure 4).

Transformation from EES-Fe_3N_2 to ESS-$Fe_3(N)_2$ was explored by scanning the potential energy surfaces of low energy sextet, octet, and decet spin state pathways (Figure 3). The scans reveal low (<5 kcal/mol) barriers for the transformation on each of the three potential-energy surfaces (see Supporting Information). Thus, calculations imply that

dx.doi.org/10.1021/ic300150u | Inorg. Chem. 2012, 51, 7546 7550

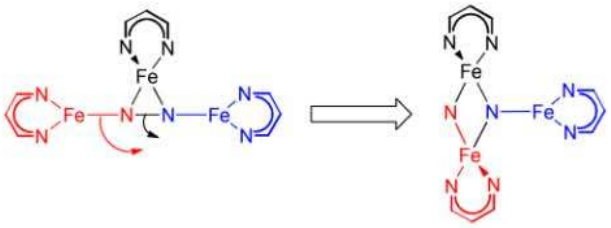

Figure 3. Potential energy scans (red/black arrows) between EES-Fe_3N_2 (left) and ESS-$Fe_3(N)_2$ (right) indicate small barriers to N_2 scission.

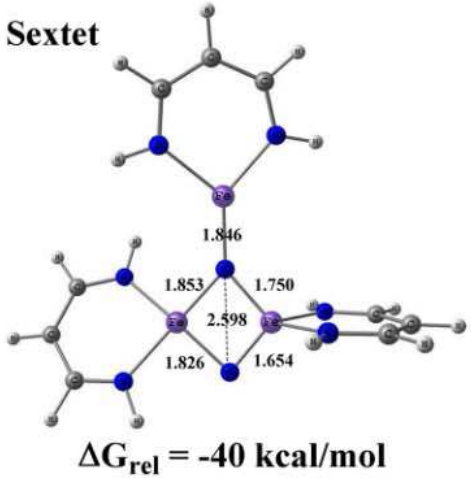

Figure 4. B3LYP calculated geometry of ^{6}ESS-$Fe_3(N)_2$ with an broken N_2 bond. (Bond lengths given in Å.) G_{rel} is calculated relative to isolated [Fe] and N_2.

isomerization could be kinetically rapid as a part of the reaction leading to N_2 cleavage, but that the N N cleavage is thermodynamically unfavorable for the neutral cluster.

Inspection of Figure 1 indicates several K^+ directly interacting with the -system of the aryl substituents and the nitrides.[8] Several potential roles of the potassium in the N N cleavage can be envisioned: K^+ may enforce geometrical constraints, stabilize the nitride (N^3), and/or increase the - backbonding capacity of the Fe centers, as proposed for the heterogeneous catalyst.[1] To assess the impact of K^+ on N_2 fixation, a K^+ ion was placed in several locations in proximity to the N_2 moiety for the low-energy dinitrogen and dinitride structures (i.e., ^{10}EES-Fe_3N_2 with an intact N_2 and ^{6}ESS-$Fe_3(N)_2$ with a broken N_2 bond), respectively. The addition of K^+ to ^{10}EES-Fe_3N_2 always rearranges upon DFT geometry optimization to the structure in Figure 5 (left). Binding of K^+ to ^{10}EES-Fe_3N_2 is exergonic by 19 kcal/mol and the calculated lowest energy multiplicity of EES-Fe_3N_2K remains a decet. The NN bond is elongated from 1.234 Å to 1.268 Å (3%) upon K^+ addition. The addition of K^+ to ^{6}ESS-$Fe_3(N)_2$ yielded the geometry in Figure 4 (right), with the sextet remaining the lowest energy spin state. The addition of K^+ to ^{6}ESS-$Fe_3(N)_2$ is 11 kcal/mol more exergonic than the K^+ addition to ^{10}EES-Fe_3N_2. Thus, the addition of K^+ stabilizes the bis(nitride) product more than the bridged N_2 complex in the gas phase. However, the nitride complex continues to have one unusually short Fe N bond.

Addition of K^+ to ^{6}ESS-$Fe_3(N)_2$ makes the resulting bis(nitride) (Figure 4) more energetically accessible, relative

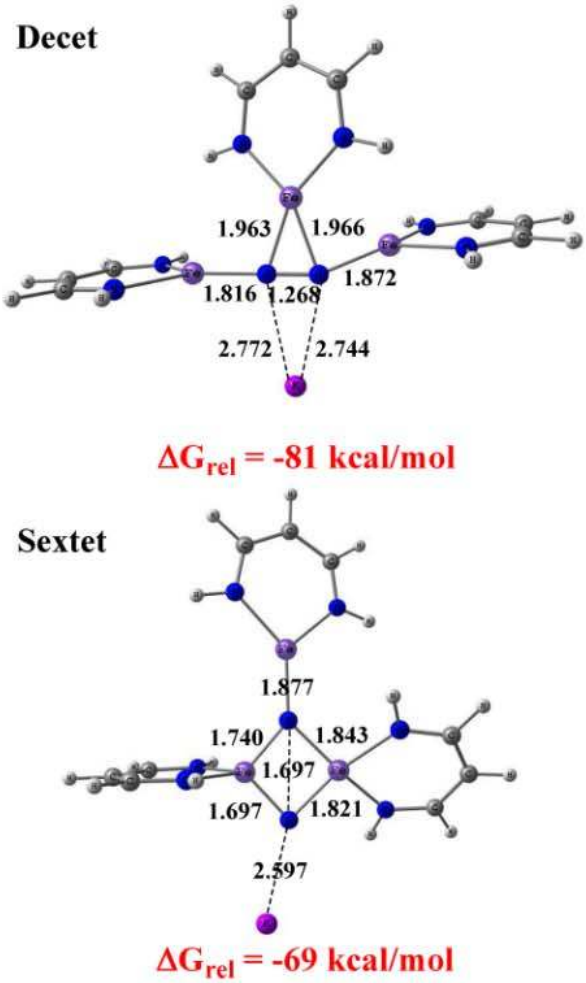

Figure 5. B3LYP structures resulting from the addition of K^+ to ^{10}EES-Fe_3N_2 (top) and ^{6}ESS-$Fe_3(N)_2$ (bottom). G_{rel} is calculated relative to isolated [Fe] and N_2.

to the dinitrogen isomers, with a free energy for the reaction ^{6}ESS-$Fe_3(N)_2K^+$ ^{10}EES-$Fe_3N_2K^+$ of only 12 kcal/mol, which is roughly half the comparable isomerization free energy in the absence of K^+. Analysis of calculated atomic charges (see the Supporting Information) suggests that greater stabilization of the N^3 ligand by K^+ coordination is responsible for the diminution of the endergonicity in the nitrogen scission reaction.

Finally, an electron was added to the ^{10}EES-Fe_3N_2 complex to mimic reduction by the fourth Fe(I) fragment in the experimental reaction. This yielded [^{9}EES-Fe_3N_2] as the lowest energy state, and resulted in only slight geometric distortion (root-mean-square deviation (rmsd) = 0.22 Å). The largest perturbation was the elongation of one Fe N bond from 1.976 Å to 2.089 Å for the [S Fe] fragment, which coincided with an increase of atomic charge on the nitrogen involved in the bond, from 0.19 to 0.58. The added electron occupies a nonbonding, Fe-based orbital, Figure 6, consistent with the minor change in geometry upon reduction. Thus, addition of a single electron to the tri-iron structure has a minor impact on the degree of N_2 activation by trimetallic EES-Fe_3N_2.

On the other hand, the addition of an electron to ^{6}ESS-$Fe_3(N)_2$ gave a significant effect. Reduction yielded [^{5}ESS-$Fe_3(N)_2$] as the lowest energy state. The distance between the

dx.doi.org/10.1021/ic300150u | Inorg. Chem. 2012, 51, 7546 7550

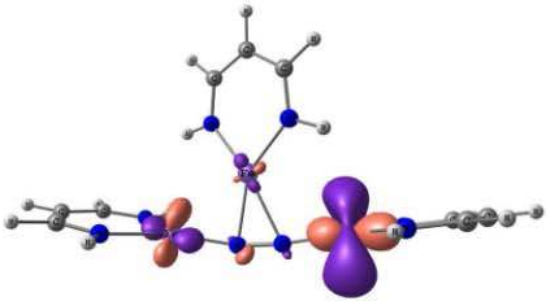

Figure 6. Highest occupied molecular orbital (HOMO) for ^{9}[EES-Fe_3N_2] complex in which the added electron occupies a nonbonding metal-based orbital.

nitride ligands is shortened from 2.598 Å to 2.587 Å. The added electron was found to occupy a bonding Fe-nitride orbital (Figure 7). A K^+ ion was added to the reduced complexes

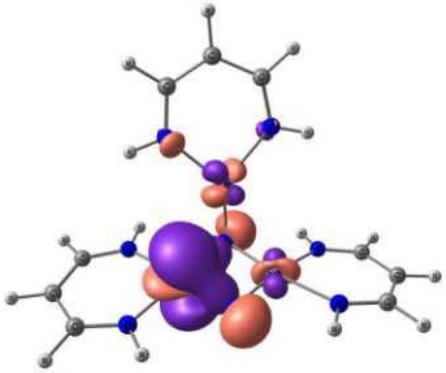

Figure 7. HOMO for [^{5}ESS-$Fe_3(N)_2$] in which the added electron occupies a bonding metal-nitride based orbital.

[^{9}EES-Fe_3N_2] and [^{5}ESS-$Fe_3(N)_2$] changing the overall charge on the cluster model to neutral; the resulting complexes were found to possess the same ground spin states as their anionic precursors (Figure 8).

The addition of K^+ to the reduced species makes the [^{5}ESS-Fe3$(N)_2$K] cluster 3 kcal/mol more stable than [^{9}EES-Fe_3N_2K] (Figure 8). It also gives a structure in which the Fe N bonds are closer to the experimental crystal structure where the Fe N bonds proximal to coordinated K^+ are shorter than the corresponding distal Fe N bond lengths. Therefore, addition of three iron(I) fragments, a K^+ ion, and an electron makes N N cleavage favorable, presumably because of the stronger interaction of the K^+ cation with the anionic nitride core.

While gas-phase simulations may more appropriately model an industrial nitrogen fixation catalyst, the inclusion of solvent effects is more pertinent to attempt to create a homogeneous version. Continuum solvation corrections in THF were thus computed and compared to the gas-phase energetics to assess the impact of solvation on the reactions of interest. The THF thermodynamics (Figure 9 (right, blue border)) are calculated to be similar to the gas-phase models with one interesting difference. The thermodynamics of ^{10}EES-Fe_3N_2 ^{6}ESS-$Fe_3(N)_2$ are changed little by the inclusion of solvent effects (G_{gas} = +22.0 kcal/mol vs G_{THF} = +21.5 kcal/mol; see Figure 9). Similarly, there is a mild solvent influence calculated for the K^+ and K-ligated reactions (e.g., ^{10}[EES-$Fe_3N_2K]^+$ ^{6}[ESS-$Fe_3(N)_2K]^+$, G_{gas} = +11.3 kcal/mol, G_{THF} = +14.9

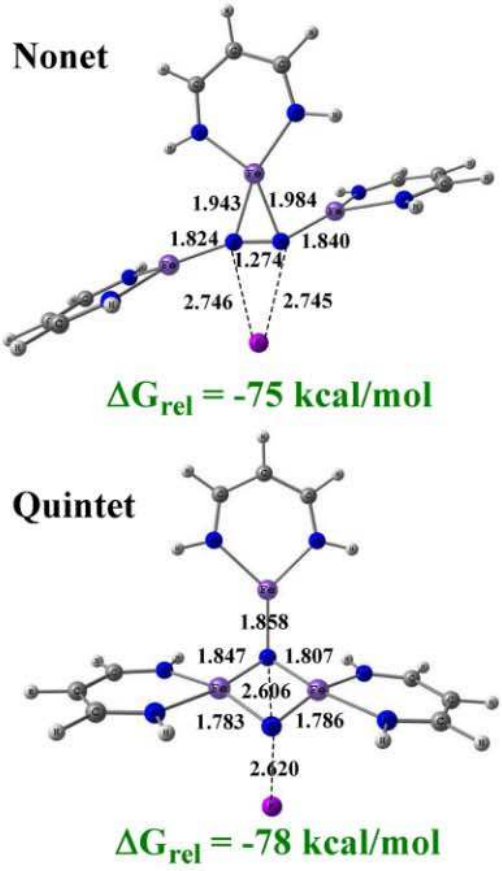

Figure 8. B3LYP structures resulting from addition of K^+ to [^{9}EES-Fe_3N_2]K (top) and [^{5}ESS-$Fe_3(N)_2$]K (bottom). G_{rel} is calculated relative to isolated [Fe], K^+, and N_2.

kcal/mol; see Figure 9). However, reduction upon the nitride-to-bis(nitride) transformation is significantly modulated by solvent, going from endergonic (G_{gas} = +8.4 kcal/mol) to mildly exergonic (G_{THF} = 0.5 kcal/mol) for ^{9}[EES-Fe_3N_2] ^{5}[ESS-$Fe_3(N)$] (see Figure 9). Comparing the relative G values in gas (G_{gas}) and solvent (G_{THF}) indicates that K^+ becomes less impactful ($G_{gas}(K^+)$ = 10.7 kcal/mol, $G_{THF}(K^+)$ = 6.6 kcal/mol) than reduction of the system (G_{gas}(e) = 13.6 kcal/mol, G_{THF}(e) = 22.0 kcal/mol) upon the inclusion of continuum THF solvent effects.

CONCLUSIONS

The present density functional theory (DFT) simulations of the sequential addition of Fe- -diketiminate fragments to dinitrogen are important because they show a reasonable series of metal binding and reduction events that cleave N_2 to give a $Fe_3(N)_2K$ core like that in a recent experimental report.[7] In addition to this mechanistic insight, it reveals that three reduced iron centers acting in a cooperative fashion make N_2 cleavage thermodynamically feasible. As summarized in Figure 9, the K^+ promoter stabilizes the nitride ligand of the fixed tri-iron-bis(nitride) isomers by 10 kcal/mol, relative to the N_2 isomers, and N N cleavage is only favorable when an added electron *and* potassium are present. However, including a polar continuum solvent reduces the impact of the K^+ on stabilizing the reduced tri-iron-bis(nitride). The results demonstrate that the cleavage of N N bonds by a reduced iron fragment is greatly influenced by potassium, and also illustrate the impact

dx.doi.org/10.1021/ic300150u | Inorg. Chem. 2012, 51, 7546 7550

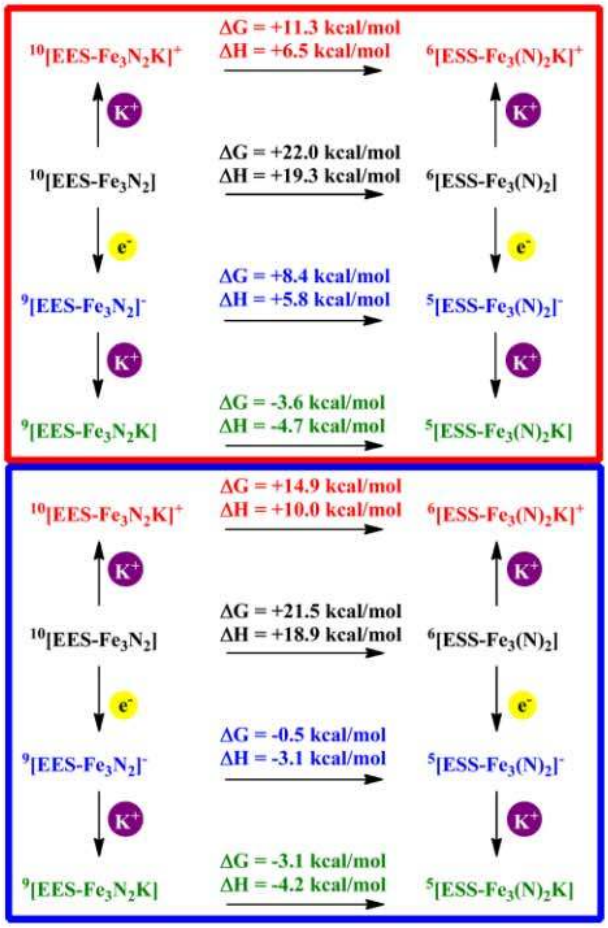

Figure 9. Ladder of calculated gas phase (red border) and solution phase (blue border) relative free energies (G_{rel}) of dinitrogen (left) and bis(nitride) (right) species. Additions of K^+ (red) and electron (blue) to the neutral species (black) are compared (G). Also, the addition of K^+ (green) to the reduced species (blue) is also calculated.

of cooperative Fe binding upon N_2 activation, indicating that at least three iron fragments are needed to cleave N_2.

ASSOCIATED CONTENT

* Supporting Information

Additional metric data, atomic charges of all calculated species, and full citation for ref 15. This material is available free of charge via the Internet at http://pubs.acs.org.

AUTHOR INFORMATION

Corresponding Author

*E-mail: t@unt.edu.

Notes

The authors declare no competing financial interest.

ACKNOWLEDGMENTS

The authors acknowledge financial support from the National Science Foundation (TRC: Nos. CHE-1057785 and CHE-0701247) and the National Institutes of Health (PLH: No. GM065313).

REFERENCES

(1) Schlogl, R. In *Handbook of Heterogeneous Catalysis*, 2nd Edition; Ertl, G., Knozinger, G., Schuth, F., Weitkamp, J., Eds.; Wiley VCH: Weinheim, Germany, 2008; *Vol. 5*, pp 2501 2575.
(2) Mittasch, A. *Geschichte der Ammoniaksynthese*; Verlag Chemie: Weinheim, Germany, 1951.
(3) Strongin, D. R.; Somorjai, G. *J. Catal.* **1988**, *109*, 51.
(4) Monillas, W. H.; Yap, G. P.; Theopold, K. H. *Inorg. Chim. Acta* **2011**, *369*, 103.
(5) Ding, K; Brennessel, W. W.; Holland, P. L. *J. Am. Chem. Soc.* **2009**, *131*, 10804.
(6) Ding, K.; Pierpont, A. W.; Brennessel, W. W.; Lukat-Rodgers, G.; Rodgers, K. R.; Cundari, T. R.; Bill, E.; Holland, P. L. *J. Am. Chem. Soc.* **2009**, *131*, 9471.
(7) Horn, B.; Pfirrmann, S.; Limberg, C.; Herwig, C.; Braun, B.; Mebs, S.; Metzinger, R. *Z. Anorg. Allg. Chem.* **2011**, *637*, 1169.
(8) Schrock, R. R. *Angew. Chem., Int. Ed.* **2008**, *47*, 5512.
(9) Khoroshun, D. V.; Musaev, D. G.; Morokuma, K. *Mol. Phys.* **2002**, *100*, 523.
(10) Cavigliasso, G.; Wilson, L.; McAlpine, S.; Attar, M.; Stranger, R.; Yates, B. F. *Dalton Trans.* **2010**, *39*, 4529.
(11) Rodriguez, M. M.; Bill, E.; Brennessel, W. W.; Holland, P. L. *Science* **2011**, *334*, 780.
(12) Bennett, M. V.; Stoian, S.; Bominaar, E. L.; Munck, E.; Holm, R. H. *J. Am. Chem. Soc.* **2006**, *127*, 12378.
(13) Bennett, M. V.; Holm, R. H. *Angew. Chem., Int. Ed.* **2006**, *45*, 5613.
(14) Strongin, D. R.; Carrazza, J.; Bare, S. R.; Somorjai, G. A. *J. Catal.* **1987**, *103*, 213.
(15) Frisch, M. J. et al.. *Gaussian 09*, Gaussian, Inc.: Wallingford, CT, 2009.
(16) Smith, J. M.; Lachicotte, R. J.; Pittard, K. A.; Cundari, T. R.; Lukat-Rodgers, G.; Rodgers, K. R.; Holland, P. L. *J. Am. Chem. Soc.* **2001**, *123*, 9222.
(17) Pierpont, A. W.; Cundari, T. R. *J. Coord. Chem.* **2011**, *64*, 3123.
(18) Smith, J. M.; Sadique, A. R.; Cundari, T. R.; Rodgers, K. R.; Lukat-Rodgers, G.; Lachicotte, R. J.; Flaschenriem, C. J.; Vela, J.; Holland, P. L. *J. Am. Chem. Soc.* **2006**, *128*, 756.
(19) Marenich, A. V.; Cramer, C. J.; Truhlar, D. G. *J. Phys. Chem.* **2009**, *113*, 6378.